Development and Testing of Hierarchically Wrinkled Coatings for Marine Antifouling

Kirill Efimenko,*,† John Finlay,‡ Maureen E. Callow,‡ James A. Callow,‡ and Jan Genzer*,†

Department of Chemical & Biomolecular Engineering, North Carolina State University, Raleigh, North Carolina 27695-7905, and School of Biosciences, University of Birmingham, Birmingham B15 2TT, U.K.

ABSTRACT We report on the formation and testing of novel marine coatings comprising hierarchically wrinkled surface topographies (HWTS) having wrinkles of different length scales (generations) ranging from tens of nanometers to a fraction of a millimeter. The individual wrinkle generations are arranged in nested patterns, where each larger wrinkle resides underneath and represents a scaled-up version of the smaller wrinkle. We present and discuss results from field tests in seawater and laboratory experiments. The results of our field tests reveal that while coatings with flat topographies foul after relatively short time periods (4−15 weeks), the HWST coatings with the same chemistries as flat coatings remain relatively free of biofouling even after prolonged exposure to seawater (18 months). In contrast to flat coatings, the HWST substrates are not colonized by barnacles. These observations suggest that surface topography plays a dominant role in governing the coating defense against barnacle fouling even without fine-tuning the chemical composition of the overcoat. Laboratory experiments indicate that settlement of zoospores of the green alga *Ulva* and the strength of attachment of sporelings (young plants) depend on the chemical composition of the coating as well as surface topography.

KEYWORDS: marine fouling • buckling • wrinkling • topographically corrugated substrate • *Ulva* settlement • barnacle settlement

INTRODUCTION

For decades, scientists and engineers have strived to find solutions to marine fouling by designing novel chemical routes that would facilitate the production of effective antifouling coatings. While success has been achieved with some biocidal antifouling coatings, it is clear, after many years of work, that it may not be possible to design an effective antifouling coating without the use of biocides (1, 2). Since biocidal antifouling is under increasing scrutiny by regulatory authorities, research has shifted in its focus and currently aims at designing and engineering fouling-release coatings, which can be cleaned by applying a weak mechanical force, such as one supplied by shear forces acting on a boat in motion (3). Recent research on antifouling or fouling-release coatings has also led to the realization that surface chemistry alone cannot offer sufficient control over the coating's characteristics. Thus, in addition to controlling surface chemistry, additional material parameters may play a noteworthy role in governing marine fouling, including (1) surface topography, (2) substrate "softness" (i.e., modulus), (3) lubricity, and (4) the dynamics of the functional groups present on the surfaces of coatings (2). Over the past few years, numerous reports have confirmed that surface topography does play a significant role in governing the settlement of marine species on man-made surfaces (4−8). Field studies by Thomason and colleagues demonstrated that recruitment of barnacles onto textured tiles depended on a number of factors, including tile size and the scale of roughness (4, 5) as well as environmental and biological factors such as gregariousness (7, 8). Some of the most comprehensive and systematic work pertaining to the use of topography in reducing marine fouling has been carried out in laboratory studies by Brennan and co-workers (9−14) and other groups (15−22). The major outcome of these studies has been a clear demonstration that the degree of biofouling of various marine organisms is closely correlated with the interplay between the size of the colonization stages of the marine species and the dimension and shape of geometrical protrusions on surfaces (as well as surface chemistry).

While a number of previous studies demonstrated conclusively the antifouling potential of topographically corrugated surfaces, the mechanisms governing the ability of surfaces to minimize fouling, i.e., reduced settlement/attachment, growth, and increased removal, are still not completely clear. Brennan and co-workers concluded that effective coatings should possess topographical features whose sizes are smaller than either the dimension of the settling stages of the marine organisms or those parts of the larvae that "explore" the surface: e.g., the antennules of a barnacle cypris larva (13, 14). De Nys and colleagues showed that adhesion can be related to the number of attachment points of the marine organism to the surface (17, 21). Ignoring momentarily the actual shape of the topographical features on the surface, one would expect that the number of attachment points is associated with the match or mismatch between the size of the organism and the characteristic topographic dimensions of the coatings. To this end, the adhesion strength of fouling organisms that are larger

* To whom correspondence should be addressed. E-mail: efimenko@ncsu.edu (K.E.); Jan_Genzer@ncsu.edu (J.G.).

Received for review January 27, 2009 and accepted March 23, 2009

† North Carolina State University.

‡ University of Birmingham.

DOI: 10.1021/am9000562

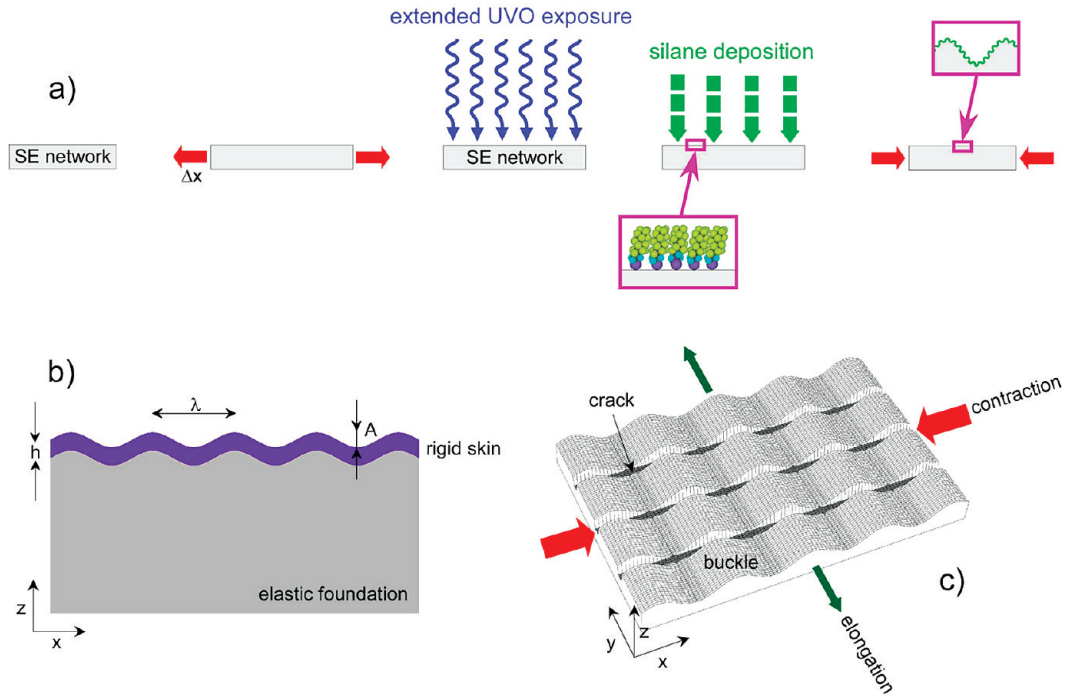

FIGURE 1. (a) Schematic depicting the technological steps leading to the formation of coatings with uniaxial hierarchically wrinkled surface topologies (uHWST). (b) Definition of the parameters of HWST surfaces comprising a thin rigid skin (thickness *h*) resting on top of an elastic foundation: *A*, wrinkle amplitude, λ, wrinkle wavelength. (c) Formation of uHWST coatings by uniaxially stretching silicone elastomer (SE) supports, i.e., PDMS, exposing them to ultraviolet/ozone treatment, a process that creates the rigid skin resting on top of an unmodified soft PDMS support, and releasing the imposed strain. The last process leads to the formation of uHWST. As a result of a positive Poisson ratio, cracks develop in samples during the strain release; these are oriented parallel to the direction of the imposed strain.

than the length scale of the surface topographical features would be reduced because fewer attachment points exist between the organism and the substrate. Conversely, organisms settling on topographically modulated surfaces with topographic features larger than the organism's dimension would attach more strongly, as there would be more attachment points available for adhesion.

Biofouling encompasses a very diverse range of marine organisms (e.g., bacteria, algae, barnacles) with settling stages that span several orders of magnitude ranging from hundreds of nanometers to centimeters. For this reason, a topographical pattern having a single length scale is unlikely to perform as a well as generic antifouling and/or fouling-release coating. Instead, surface corrugations having multiple length scales acting in concert should be utilized in the design of an effective antifouling surface. In this paper we describe the fabrication of such coatings that comprise hierarchically patterned topographies with dimensions ranging from nanometers to millimeters. We present and discuss the results of field tests performed in seawater as well as laboratory assays with a common fouling macroalga, *Ulva*. Specifically, we have prepared a coating comprising hierarchical wrinkles in a poly(dimethylsiloxane) base layer and tune their surface chemical composition by organosilane and polymeric amphiphilic layers. Two types of wrinkled geometries are explored in which the wrinkles are oriented either uniaxially or biaxially. We will demonstrate that, while not yet fully optimized, such coatings may represent a promising new platform for fabricating efficient fouling-release marine coatings.

MATERIALS AND METHODS

Preparation of Flat Substrates. Flat substrates for this study were prepared from a commercial poly(dimethylsiloxane) (PDMS) kit, Sylgard-184 (Dow Corning), following the procedure suggested by the manufacturer. Self-standing PDMS films (thickness of ~500 μm) were first modified with ultraviolet/ozone (UVO) treatment for 30−35 min, which rendered the surface hydrophilic (23). Such PDMS films were further treated with one of three different surface modifications. In one of them, the UVO-modified surfaces were decorated with a self-assembled monolayer (SAM) made of 1*H*,1*H*,2*H*,2*H*-perfluorodecyltrichlorosilane (tF8H2, Gelest) that was applied via vapor deposition for 15 min, followed by washing the substrates copiously with ethanol (in order to remove any weakly physisorbed tF8H2) and drying with nitrogen gas. The second set of substrates was prepared by spin-coating a film of poly(2-hydroxyethyl methacrylate) (PHEMA), synthesized by free radical polymerization, from 2% solutions in methanol onto UVO-modified PDMS and annealing the sample at 70 °C for 72 h. The thickness of the PHEMA layer was approximately 50−70 nm, as determined from ellipsometry measured on PHEMA-coated silicon wafer substrates. In the third set of experiments we repeated the procedure from the previous set and exposed the PHEMA-coated substrate after annealing to tF8H2 vapor for 15 min. The samples were subsequently washed with ethanol and dried with nitrogen gas.

Preparation of Hierarchically Wrinkled Surfaces. Specimens with uniaxial hierarchically wrinkled surface topographies (uHWST) were fabricated using the methodology developed by Efimenko and co-workers (24); the process is shown schematically in Figure 1a. After a PDMS flat sheet was mounted into a stretching device, a uniaxial strain, Δx ($\Delta x = 30\%$ in this work), was applied. The substrate was then exposed to the UVO treatment for 30 min. Subsequently, the sample was exposed to the vapor of tF8H2 for 15 min and the strain was released

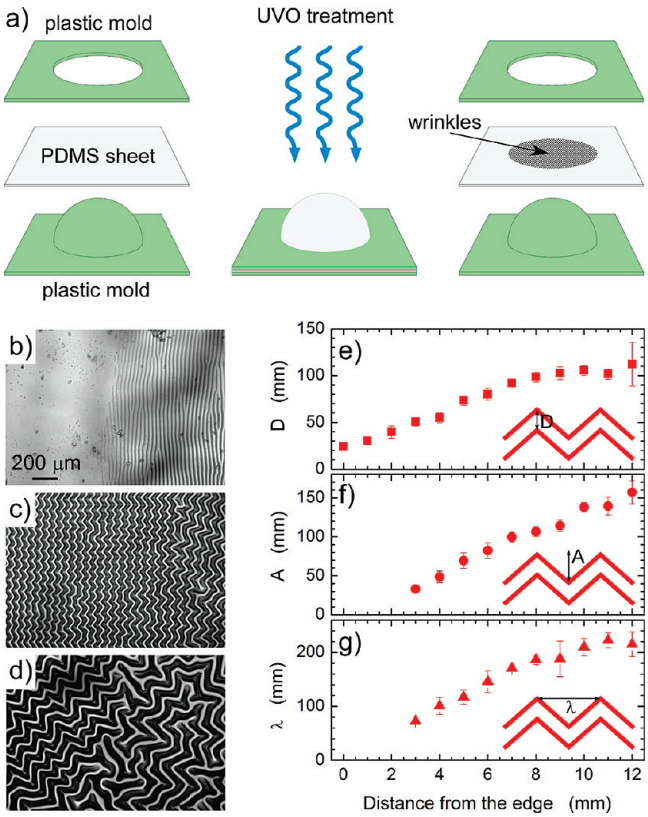

FIGURE 2. (a) Schematic illustrating the formation and properties of biaxial hierarchically wrinkled surface topologies (bHWST). (b)–(d) Optical micrographs of the bHWST taken at different location along the sample (b, close to the edge, c, halfway between the edge and the center; d, center). (e)–(g) variation of the wrinkle geometrical features (defined in the insets) as a function of the position along the substrate (0, edge; 12.5 mm, center). The scale bars in (c) and (d) are identical with that in (b).

from the sample. As discussed in the original publication (24), the latter process resulted in the formation of HWST substrates comprising wrinkles of five distinct periodicities ranging from a few nanometers to a fraction of a millimeter; the individual wrinkle generations were organized such that smaller wrinkles rested on top of larger wrinkles. In an alternative procedure, the tF8H2 deposition was carried out after the strain was released from the sample. In our test, we did not detect any difference between the substrates fabricated by the two methods. In addition to tF8H2-covered substrates, HWST specimens were prepared that were covered with PHEMA and PHEMA/tF8H2 coatings. These coatings were applied on the HWST samples using the procedure discussed earlier.

We have also prepared coatings with biaxial wrinkle topographies (bHWST). Those were generated by following the procedure that is schematically depicted in Figure 2a. A flat sheet of PDMS was stretched over a support containing a hemispherical protrusion. After the UVO treatment (30 min), the substrate was removed from the assembly; the wrinkling pattern was present in a circular area (diameter ~25 mm). In this biaxial stretching geometry, the surface topographies consist of three wrinkling patterns. Close to the edge circular uniaxial pattern aligned parallel to the edge can be found (Figure 2b). The center of the circular wrinkled regions is covered with disordered wrinkles (Figure 2d). Wrinkles that reside between the uniaxial and disordered geometries adopt chevron-type patterns (Figure 2c); such geometries have been reported previously (25, 26). The variations of the sizes of the three structural characteristics of the chevrons with their definition are plotted in Figure 2e–g as a function of the position of the distance from the edge of the wrinkling pattern. A fraction of samples was decorated with the tF8H2 monolayers using the method described earlier. The biaxial strain was estimated to be ≈20%.

Mounting Coatings onto Solid Supports. For the field and laboratory tests, the samples were mounted onto flat solid supports. Field test specimens were first cut into 15 × 30 cm^2 dimensions and attached to polycarbonate sheets via epoxy glue. Prior to attachment, the back side of the coating was briefly exposed to UVO treatment (~3 min) in order to generate a sufficient number of hydrophilic groups that would facilitate good adhesion of the coating with the epoxy glue. The samples for laboratory experiments were cut into 2.5 cm × 7.5 cm dimensions, exposed briefly (~3 min) to UVO and attached to microscope glass slides via Correz Flex™ adhesive (Microphase Coatings) or by depositing a drop of PDMS without a cross-linker and briefly exposing it to UVO. Neither of the adhesive materials was found to cause detrimental effects to the marine test organisms.

Field Tests in Seawater. The field tests were performed during the time period from April 2005 until October 2006 at the Microphase Coatings testing site located at Wrightsville Beach (34° 13′ N, 77° 48′ W) near Wilmington, NC. The samples mounted onto polycarbonate supports were lowered into seawater at depths of about 1 m below the surface, facing the open ocean. The samples were not caged. After different periods of time, the samples were removed, photographed, washed with a stream of fresh water aimed perpendicularly to the substrate (distance ~20 cm), and photographed again.

Settlement and Adhesion Assays with Zoospores of *Ulva.* Samples were immersed in distilled water for 24 h and then transferred to artificial seawater (ASW) for 1 h prior to the start of the experiments.

Zoospores were released from fertile plants of *Ulva linza* and prepared for assays as described previously (27). In brief, 10 mL of zoospore suspension was pipetted into individual compartments of polystyrene Quadriperm culture dishes (Greiner) each containing a glass microscope slide. The dishes were incubated in darkness at approximately 20 °C. After 1 h the slides were gently washed in seawater to remove zoospores that had not attached. After fixation in glutaraldehyde, the density of zoospores attached to the surface was counted on each of three replicate slides using an image analysis system attached to a fluorescence microscope (9). Spores were visualized by autofluorescence of chlorophyll. Counts were made for 30 fields of view (each 0.17 mm^2) on each of 3 replicate slides.

Spore counts on the biaxially HWST samples were obtained from 30 random fields of view on each of 4 replicate samples. The strength of attachment of spores was determined by exposing replicate samples to an impact pressure of 132 kPa generated by an automated water jet (28, 29). Surfaces remained wetted during fixing of slides to the support prior to exposure to water jet. The percentage removal was calculated from the difference between samples before and after exposure to the water jet.

Adhesion Assays with Sporelings of *Ulva.* Spores were allowed to settle as described above. After unsettled spores were washed away, the attached spores were cultured in enriched seawater medium in Quadriperm dishes as described in ref 29. The medium was refreshed every 2 days, and the sporelings were cultured for 8 days. Sporeling biomass was determined in situ by measuring the fluorescence of the chlorophyll, as relative fluorescence units (RFU), contained within the sporelings using a Tecan fluorescent plate reader. The RFU value for each slide is the mean of 196 point fluorescence readings. The strength of attachment of sporelings was quantified after exposure to a wall shear stress of 53 Pa generated in a custom-built flow channel (30). The surfaces remained wet during fixing the slides in the flow channel. This method was used for

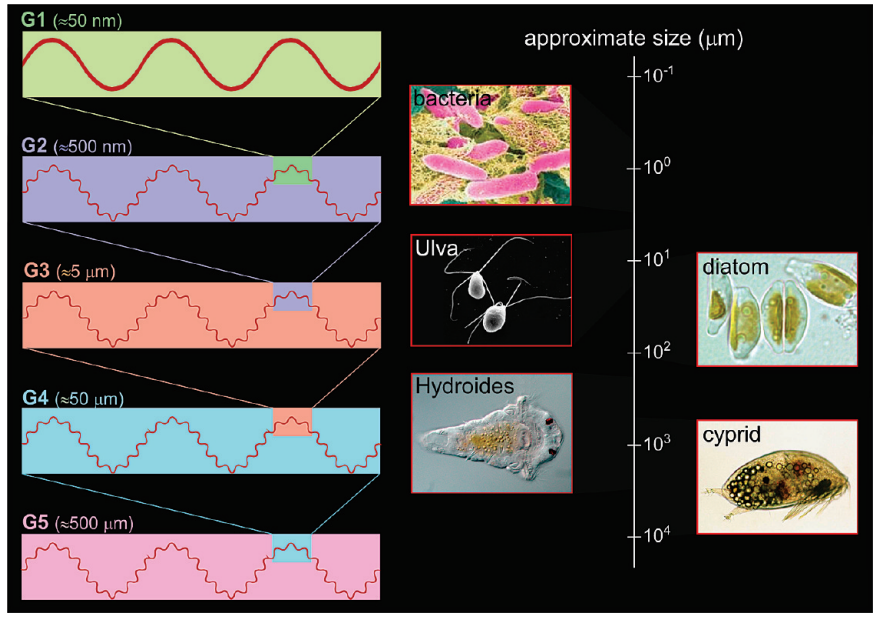

FIGURE 3. Schematic depicting the structure of HWST coatings comprising nested wrinkled topographies ranging from tens of nanometers to a fraction of a millimeter. The right panel shows typical dimensions of selected marine organisms. Credits: *Hydroides elegans* larva (B. Nedved, University of Hawaii, USA), *Balanus amphitrite* cyprid (A. S. Clare, University of Newcastle, U.K.)

sporelings, as their adhesion strength is lower than that of zoospores (31, 32). An additional standard of PDMS, Silatic T2 (Dow Corning), was included for comparative purposes, since it shows good release properties for sporelings of *Ulva* (33).

RESULTS

Coating Formation. In our previous publication we have reported on the formation of surfaces comprising uniaxial HWSTs (uHWSTs) on elastomeric supports (24). In the original work we described the mechanism leading to the production of such uHWST patterns by invoking a simple model that explains wrinkling/buckling as a result of the competition between the bending-dominated deformations of a rigid skin resting on an infinitely thick soft foundation. The thin skin on top of soft silicone elastomer foundation, i.e., PDMS, is formed by exposing the PDMS network to UVO treatment for extended periods of time (tens of minutes). Efimenko and co-workers reported that the thickness of the skin, whose electron density is ~50% of that of silica, is ~5 nm (23). The stretching/shearing-dominated deformations of the substrate cause the skin to wrinkle in response to the relaxation of the applied strain, attaining a characteristic wavelength, $\lambda \approx h(E_s/E_f)^{1/3}$, where h is the thickness of the skin and E_s and E_f are the elastic moduli of the skin and the foundation, respectively (Figure 1b). Using experimentally measured values of E_s/E_f (nanoindentation) and h (X-ray reflectivity), we have established that upon releasing the strain from the sample, the first generation of wrinkles (G1) appeared, which formed an "effective skin" that was thicker and much stiffer than the original skin. Upon further release of strain from the sample, a new generation (G2) of wrinkles formed that had a larger wavelength and amplitude. The formation of higher generations of wrinkles continued until the strain was completely removed from the substrate. For strains in the range of 30−70%, we established that up to five generations of wrinkles can be formed, thus producing a hierarchically nested wrinkled pattern, where each wrinkle was a scaled-up version of the primary wrinkle (Figure 3, left panel). Efimenko and co-workers further reported that the strain release from the sample was accompanied with the formation of structural defects: i.e., typical layered dislocations and cracks. The latter structures (Figure 1c) resulted from the finite value of the Poisson ratio in PDMS ($\nu \approx 0.5$). The interplay between the density of dislocations and cracks in the sample was found to depend on the rate of strain release. To this end, the density of dislocations increased and that of the cracks decreased with increasing strain release rates; the opposite trend was observed when the strain was released relatively slowly (~50 μm/min).

Seawater Field Marine Fouling Tests. In order for the substrate to act as an effective antifouling coating, its roughness should be smaller than the size of the settling cell/organism. Having multiple length scales of topographies, one would expect that a coating that possesses HWSTs should be effective in preventing fouling of a broad range of marine organisms (Figure 3). However, it should be noted that the relevant scale may not be that of the size of the whole organism: e.g., the antennules of the cyprid of *B. amphitrite* are only ~20 μm in width, while the whole cyprid is ~500 μm. We performed two series of tests. The first one involved a long-term field immersion test in seawater, and the second aimed at establishing the performance of HWST coatings in laboratory experiments. In Figure 4 we reproduce photographs of uHWST coatings after removing them from seawater (upper panel) and after cleaning them with a garden hose water jet held perpendicular to the sample surface (lower panel). Visual assessment of the images shown in Figure 4 revealed some interesting trends. Even after 1 month of seawater immersion, the flat samples were fouled considerably. The fouling was not removed after extensive washing with a stream of water (bottom panels). After more

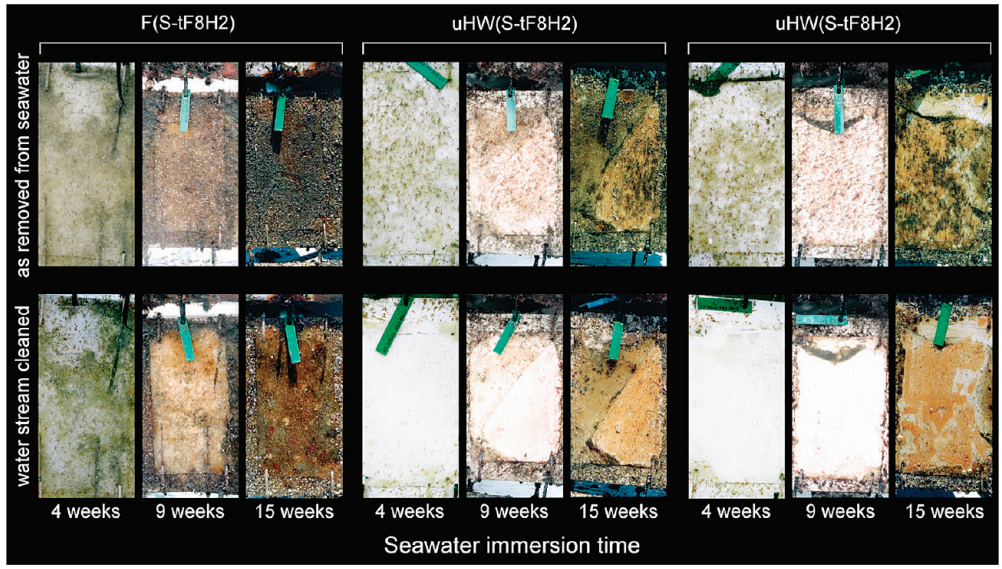

FIGURE 4. Images of marine coatings comprising flat PDMS (left panel) and uHWST (middle and right panels) sheets covered with a SAM made of tF8H2 after immersion in seawater (April−August 2005, Wilmington, NC) for various times. The sample set shown in the middle panel had tF8H2 deposited onto prestretched substrate before releasing the strain. The right panel represents substrates that were decorated with tF8H2 SAMs after the strain was removed from the specimens. The upper row shows images of specimens immediately after the removal from the seawater, and the bottom row depicts samples after washing with a water stream.

than 1 month exposure in the sea, the fouling progressively worsened (images not shown). The performance of uHWST specimens was different from that of the flat samples; the uHWST coatings remained relatively clean even after extensive immersion times in seawater. Most of the deposits found immediately after sample removal were successfully cleaned off by spraying the specimens with a jet of water. There was no visible difference between the two series of the uHWST samples. The images of the uHWST coatings taken after 15 weeks revealed that while some samples delaminated from the polycarbonate supports, the modified surfaces remained relatively clean. More detailed imaging was performed on the samples that completely delaminated from the supports after 15 weeks (series of samples prepared by depositing the tF8H2 organosilane after the formation of hierarchical wrinkles). The specimens were placed into standing water for 24 h and subsequently gently swept with a Kimwipe. Because only one sample was available from each series, the analysis that follows reveals average deposits determined from different areas on one sample. Optical microscopy imaging revealed that the uHWST coatings remained relatively clean; only a few spots on the sample, primarily those that contained a large fraction of structural defects, revealed the presence of diatoms. The diatom density was determined to be 615 ± 480 cells mm^{-2} of the surface projected area (the error represents the standard deviation determined by averaging 10 measurements on different areas of the same sample). The specimens that stayed attached to the polycarbonate support were kept in the seawater for an additional 14 months, and their surfaces were examined afterward after letting them stand in water for 24 h and gently rubbing them with a water-soaked Kimwipe. While there were no major differences observed in the two sets of samples (15 weeks vs nearly 18 months), the latter sample series that remained in the seawater for the entire duration of the experiment exhibited a substantial increase of the density of cracks (Figure 5a). These ran randomly across the sample; we could not distinguish them from the "expected" cracks formed during the strain release, as described earlier in the paper. In addition, more diatom deposits were found in these coatings. While the top surfaces of the wrinkles remained clean (Figure 5b), large deposits of diatoms were detected between the wrinkles ("wrinkle valleys") (Figure 5c). The diatom density estimated from the optical microscopy images was 1825 ± 596 mm^{-2} of the surface projected area; these diatoms were presumably trapped in the confined wrinkled spaces and could not be freed even after rubbing the surfaces of the coatings.

One distinctive difference between the flat coatings and those decorated with the uHWSTs was their response to barnacle settlement and growth. The flat surfaces started to exhibit barnacle recruitment after approximately 2 months in seawater. However, no barnacles were found on the uHWST coatings even after 16 months of immersion. There was one notable exception; a single barnacle was found on one of the coatings that delaminated after 2 months. A close inspection of the coating from the back side revealed that the barnacle grew on a position on the substrate that had a large structural defect. After the barnacle was removed from the substrate, the back side of the barnacle was imaged with optical microscopy (Figure 5d). From the image in Figure 5d it is evident that the wrinkled topologies "imprinted" into the base of the barnacle. We could not determine, however, how many wrinkle generations were reproduced into the barnacle base.

Laboratory Marine Fouling Tests. In addition to the field test, we also carried out a series of laboratory experiments to understand which factors are important for the settlement of zoospores of the green alga *Ulva*. The experi-

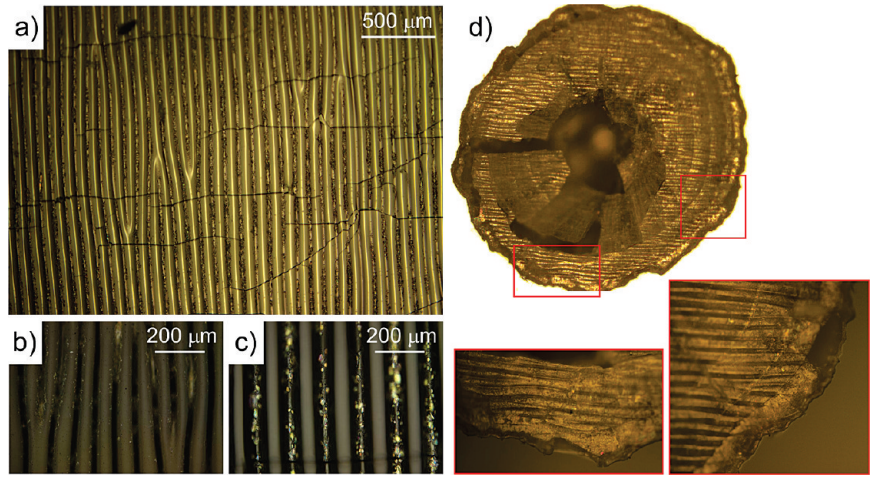

FIGURE 5. a) Photograph of a uHWST coating covered with a SAM made of tF8H2 after immersion in seawater for 18 months (April 2005−October 2006, Wilmington, NC). Parts (b) and (c) depict zoom-ins into picture (a) focusing on top (b) and bottom (c) of the wrinkled topography. (d) Photograph of a barnacle growing on top of an uHWST coating covered with a tF8H2 SAM. The coating was exposed to seawater during April−August 2005 (Wilmington, NC). The barnacle was found to grow on a defect site on the sample; it was removed gently from the substrate. Note that the wrinkled topology was "imprinted" into the barnacle base.

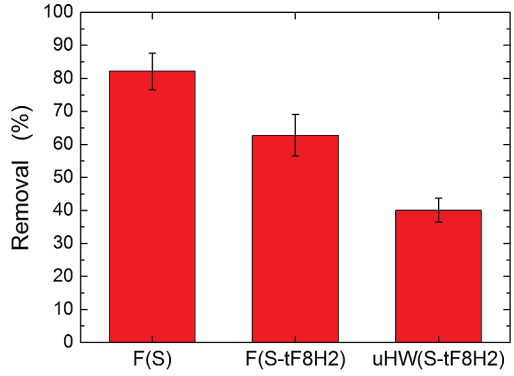

FIGURE 6. Removal of sporelings of *Ulva* from various substrates: F(S), flat Sylgard-184; F(S-tF8H2), flat Sylgard-184/tF8H2; uHW(S-tF8H2), uniaxial HWST Sylgard-184/tF8H2. The thickness of the Sylgard-184 was ~800 μm. The removal of sporelings was accomplished in a water channel at a wall shear stress of 53 Pa. Each point is the mean removal from five replicate slides. Bars represent the standard error of the mean derived from arc-sine transformed data.

ments to quantify adhesion strength (measured as percent removal) of sporelings growing on the same samples used in the field trial are described first, followed by spore attachment data and sporeling adhesion strength data for uniaxially stretched amphiphilic chemistries. Finally, spore settlement and adhesion strength on novel biaxially stretched samples are described.

The percent removal of sporelings (young plants) of *Ulva* from smooth Sylgard-184, smooth hydrophobic and uniaxially stretched hydrophobic surfaces following exposure in a flow channel to a wall shear stress of 53 Pa is shown in Figure 6. One-way analysis of variance ($F_{2,12} = 17.7$, $P < 0.05$) confirmed that sporelings were most weakly attached to the smooth PDMS and attachment strength was higher on the wrinkled than on the smooth fluorinated surface. Examination of the wrinkled surface showed that spores settled preferentially in wrinkles and cracks, which resulted in low removal of sporelings from this surface. A more comprehensive description is provided later in the Discussion.

In order to improve the release characteristics, surfaces with combined fluorine based and ethylene oxide based chemistries were examined. In Figure 7 we plot (a) spore settlement and (b) the removal of sporelings (young plants) from substrates comprising different combinations of the surface topography (stretched uniaxially) and chemistry. One-way analysis of variance ($F_{5,534} = 128.6$, $P < 0.05$) with the Tukey test showed that spore settlement density was lowest on the wrinkled fluorinated and the smooth and wrinkled amphiphilic surfaces (Figure 7a). The highest density of spores was associated with the uHWST PHEMA surface, which also had poor sporeling release properties (Figure 8b). The HW fluorinated surface possessed release properties that were comparable to those of the PDMS standard, Silastic T2. The percent removal of sporelings from the hydrophilic and amphiphilic surfaces was low (≤30%), irrespective of whether they were flat or wrinkled. One-way analysis of variance ($F_{5,24} = 6.7$, $P < 0.05$) and Tukey tests showed that the release of sporelings from the HWST PHEMA-tF8H2 substrate was not significantly different from that from flat PHEMA.

Spore settlement density and percent removal of spores by exposure to an impact pressure of 132 kPa from a water jet are shown in Figure 8 for smooth and bHWST surfaces. One-way analysis of variance and Tukey tests showed that spore settlement densities on the two UVO-treated surfaces were not significantly different but that settlement densities on the other coatings were all significantly different ($F_{4,595} = 128$, $P < 0.05$). Of the three smooth surfaces, the highest density of settled spores was found on Sylgard-184 and the lowest density on the UVO-treated sample. The highest number of spores settled on the bHWST fluorinated surface, more than double on the smooth surface of equivalent chemistry. Spores settled preferentially in depressions (Figure 9b−d). Spore removal was high from the flat PDMS-UVO, flat fluorinated, and the bHWST-UVO surfaces. Removal was not significantly different from any of these three surfaces (determined by using one-way ANOVA and Tukey

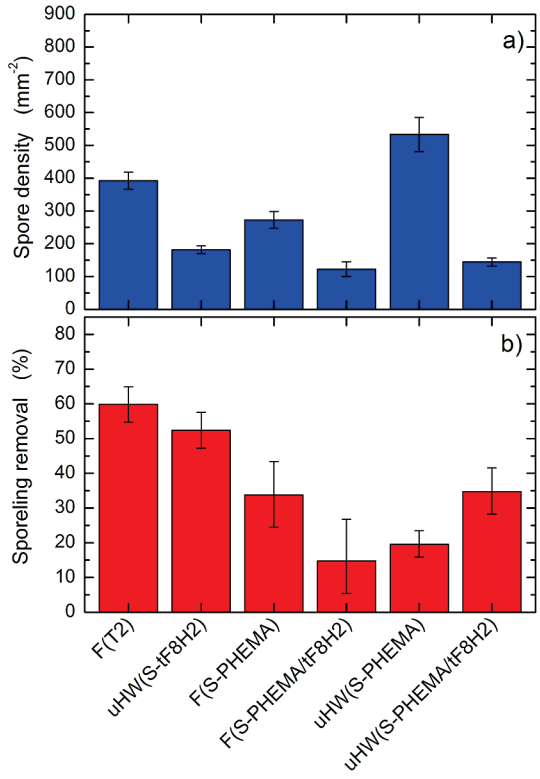

FIGURE 7. (a) Settlement of zoospores on and (b) removal of sporelings of *Ulva* from various substrates: F(T2), flat Silastic T2; uHW(S-tF8H2), uniaxial HWST Sylgard-184/tF8H2; F(S-PHEMA), flat Sylgard-184/PHEMA; F(S-PHEMA/tF8H2), flat Sylgard-184/PHEMA-tF8H2; uHW(S-PHEMA), uniaxial HWST Sylgard-184/PHEMA; uHW(S-PHEMA/tF8H2), uniaxial HWST Sylgard-184/PHEMA-tF8H2. The thickness of the Sylgard-184 was ~500 μm. The removal of sporelings was accomplished in a water channel at a wall shear stress of 53 Pa. Points in (a) represent the mean of 90 counts, 30 from each of 3 replicate slides. Bars show 95% confidence limits. Points in (b) show mean removal from 5 replicate slides. Bars represent the standard error of the mean derived from arc-sine transformed data.

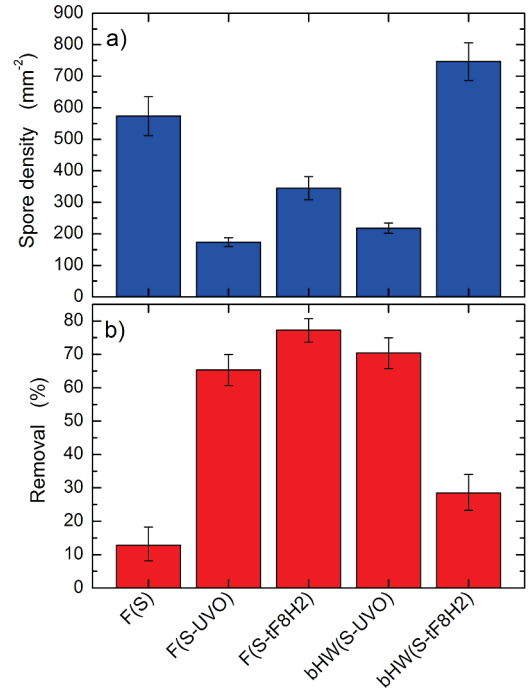

FIGURE 8. (a) Settlement of zoospores and (b) removal of zoospores of *Ulva* from various substrates: F(S), flat Sylgard-184; F(S-UVO), flat Sylgard-184 after UVO treatment; F(S-tF8H2), flat Sylgard-184/tF8H2; bHW(S-UVO), biaxial HWST Sylgard-184 after UVO treatment; bHW(S-tF8H2), biaxial HWST Sylgard-184/tF8H2. The thickness of the Sylgard-184 was ~500 μm. The removal of spores was accomplished by exposure to a water impact pressure of 132 kPa. Points represent the mean of 120 counts, 30 from each of 4 replicate slides, taken from random fields of view across the whole area of the biaxially stretched samples. Bars show 95% confidence limits. Bars on the percentage data in (b) are derived from arc-sine transformed data.

tests ($F_{4,595} = 100$, $P < 0.05$)). The combination of chemistry (UVO treatment) and biaxial wrinkles in bHW(S-UVO) produced a surface which inhibited spore settlement and promoted release characteristics. While it is difficult to deconvolute the effect of topography and chemistry, it appears that substrate hydrophilicity plays a major role in inhibiting spore settlement.

DISCUSSION

In this paper we describe the formation of hierarchically wrinkled surface topology (HWST) coatings and test their performance in both field and laboratory tests. The specific aim was to detect whether the multiple levels of roughness present on top of the coatings inhibited settlement (attachment) and growth of marine organisms. Coatings with two levels of roughness were tested by Schumacher and coworkers (14) against the settlement of spores of *Ulva* and barnacle cyprids; their results provided encouraging evidence that different scales of roughness would inhibit settlement of the two species. However, their first attempt to combine the two levels of roughness showed that that enhanced numbers of spores of *Ulva* settled on the hierarchical surfaces, because the larger features that inhibited settlement of cyprids provided attractive settlement sites for the smaller spores.

The field tests carried out with the HWST samples enabled us to make some interesting observations. While the chemistry of the coatings was not optimal (see below), our tests revealed that HWST coatings performed better than those that possessed flat topographies. The flat surfaces were seen to foul extensively after 1 month in seawater, whereas the HWST coatings remained relatively clean for more than 1 year and any deposits could be removed easily. However, while the topmost layers of the coatings could be cleaned completely (Figure 5b), some deposits, primarily of diatoms, remained trapped in the "valleys" of the wrinkles (Figure 5c). One striking difference between the two types of coatings was their dissimilar affinity toward barnacle recruitment. While barnacles were detected on the flat substrates after 15 weeks, no barnacles were present on the HWST coating even after more than 12 months of seawater immersion. The absence of barnacles on the HWST coatings may be a consequence of the inhibition of settlement by cyprid larvae or loss of juvenile and adult barnacles (see ref 34 for a review of barnacle settlement). Since the samples were not caged, the possibility that "cleaning" was mediated by grazing by fish cannot be excluded (35). Even if grazing accounts for the results, our findings suggest that barnacle adhesion on HWST surfaces is much weaker than that on flat coatings.

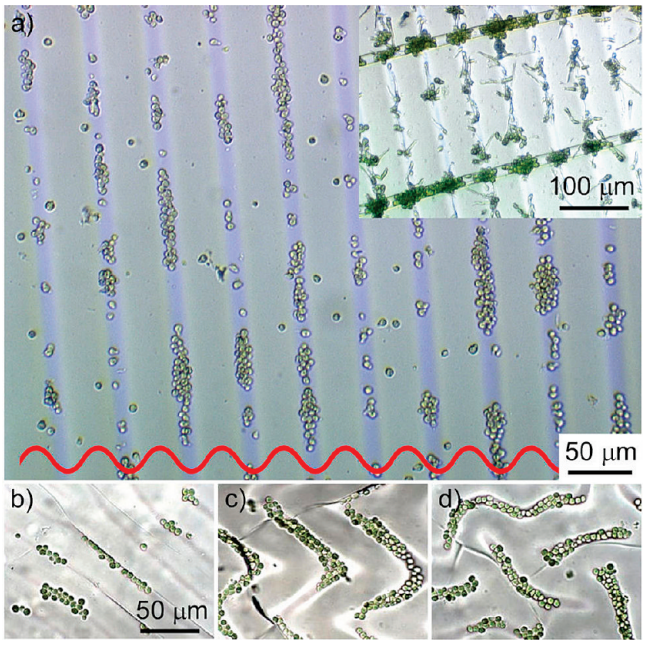

FIGURE 9. Image of zoospores settled on top of uHW(S-tF8H2) (a) and bHW(S-tF8H2) (b)−(d) substrates. The spores have settled preferentially in the wrinkle valleys (and cracks) present in uHW-(S-tF8H2) specimens. The inset shows sporelings on the surface after exposure to a wall shear stress of 53 kPa in a flow channel. Sporelings are retained in the cracks and, to a lesser extent, in the wrinkle valleys. For details of *Ulva* settlement in cracks, see the inset to (a). The positions of wrinkle "hills" and "valleys" in uniaxial HW substrates are denoted schematically by the profile shown on the bottom of (a). The bottom row denotes settlement on various locations along the biaxially buckled sample (b, close to the edge; c, halfway between the edge and the center; d, center). See Figure 2 for details of the substrate morphologies.

While more work still needs to be done in order to verify these results, our observation confirms that the coating topography plays a major role in controlling barnacle fouling on surfaces.

Concurrently with the field tests, laboratory experiments were conducted that aimed at understanding the settlement of zoospores of the green alga *Ulva* and the ease of removal of sporelings (young plants). Initially, we tested the fouling release performance of coatings on the basis of the same chemistries and same topographies as those used in the field experiments. Our results did not show an improvement in the release of sporelings relative to flat silicone elastomer coatings. Microscopic observation revealed that spores settled preferentially in the wrinkles and the cracks that developed during the stretching procedure. Spores have been shown to settle preferentially in depressions, especially when the dimensions are similar in size to those of the spore body (11, 12). Although the mature plants of *Ulva* are classed as macrofouling organisms, the settling stage, i.e., spores, is within the size range of cells referred to as microfouling. Once spores have settled in the valleys (Figure 9), they are protected from the hydrodynamic forces used to "clean" the samples. The laboratory data for *Ulva* thus concur with the observations of the field samples, which showed the accumulation and resistance to cleaning of diatoms in valleys of the uHWST samples. Furthermore, the valleys also provide shelter for the rhizoids ("roots") of the sporelings of *Ulva* as they develop, thus counteracting the fouling-release properties of the flat surface.

It is important to note that while the topography clearly plays some role in controlling the fouling of barnacles, the combination of surface topography and surface chemistry may also be important when considering fouling of smaller marine organisms. All coatings discussed thus far have been decorated with a thin layer of a semifluorinated surfactant, tF8H2, which was chemisorbed onto the surface and formed well-organized SAM films. Although fluorine chemistry has been paramount in designing superhydrophobic surfaces (1), it may not represent the best overcoat to inhibit settlement and adhesion. Furthermore, it is well-known that highly hydrophobic surfaces are not the best candidates for designing efficient protein-repellent coatings. In order to ascertain the influence of chemical composition of the coatings used in this study, we performed preliminary experiments using (1) protein-repellent PHEMA layers (36) deposited directly onto the UVO-modified PDMS and (2) amphiphilic layers comprising PHEMA films decorated with semifluorinated tF8H2 moieties (PHEMA/tF8H2). The design of the latter set of samples was motivated by recent work (37, 38), which reported that coatings composed of mixtures of ethylene oxide and semifluorinated groups exhibited an enhanced ability toward minimizing spore settlement on and enhancing cleaning of marine coatings. Our findings revealed that while coatings with flat topologies containing either PHEMA or PHEMA/tF8H2 overcoats reduced the amount of spores that settled, the latter being more effective, the removal of sporelings from the substrates relative to a bare silicone elastomer standards was reduced: i.e., adhesion strength was higher on the experimental coatings. As discussed earlier, the results were affected by settlement in valleys and cracks as shown in Figure 9a.

Much more systematic work needs to be done to establish the precise combination of physicochemical parameters that fine-tune the coating performance. As pointed out by Gudipati and co-workers, the performance of their amphiphilic coatings depended crucially on the substrate composition (37). What needs to be established in our case is the optimal concentration of the tF8H2 moieties attached to the PHEMA supporting "primer". The quality of PHEMA primers deposited onto UVO-modified supports has to also be considered. In the samples prepared for this study, we have created such layers by spin-coating PHEMA that was polymerized ex situ. One possible avenue, currently under investigation, would be to form the PHEMA/tF8H2 layer directly on the PDMS-UVO substrate by mixing HEMA monomer with tF8H2 and carrying out the polymerization reaction via free radical polymerization (initiated by adding a minute amount of initiator, i.e. AIBN, or directly by UV light). This method allows us to (1) coat conformally the HWST support without losing any structural features presented at small length scales and (2) control readily the chemical composition of the amphiphilic overcoat. Recent experiments (39) reveal that such coatings can be fabricated; moreover, they do not decompose when exposed to solutions of various pH (40).

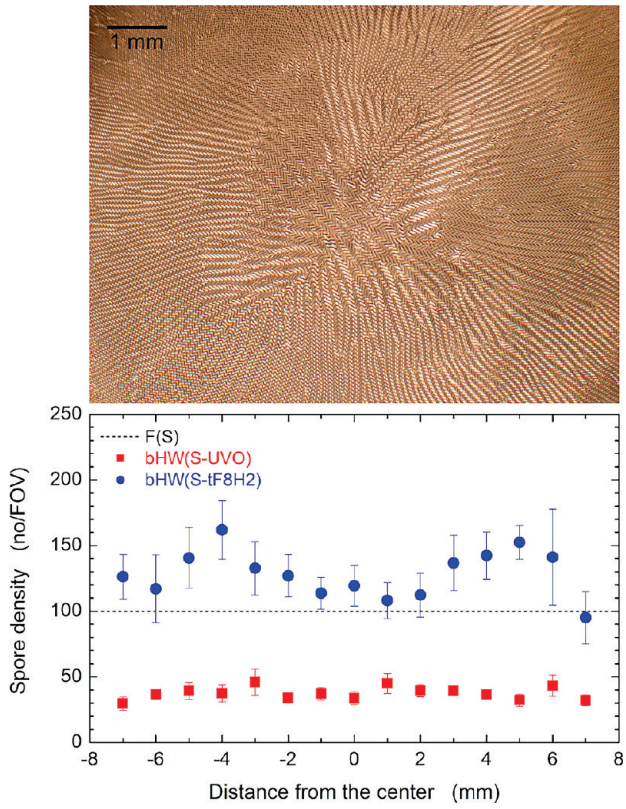

FIGURE 10. (top) Optical micrograph of a sample with biaxial hierarchically wrinkled surface topography (bHWST). (bottom) Density of attached zoospores after 1 h settlement (in number per field of view, no/FOV) on bHWST(S-UVO) (squares) and bHWST(S-tF8H2) (circles) following transects across the diameter of the patterned area. The middle of the circular pattern is shown as zero. Each point is the mean from eight transects. Bars show standard error of the mean. The dotted line represents the spore density on the flat Sylgard-184 specimen.

We attribute the latter observation to the fact that even if the C−O−Si bonds cleave, HEMA and tF8H2 form chains of individual networks (PHEMA and "polymerized" tF8H2) that are mutually interlocked. Finally, fine-tuning the properties of the HWST substrates themselves is needed. To this end, varying the UVO time, strain extent, strain release rate, strain direction, and sample dimension will be among the parameters of interest. Adjusting the UVO time and strain extent will allow for tailoring the dimension and number of generations of wrinkles. Strain release rate is known to dictate the number of structural defects and the density cracks (Figure 1c) in the coating. These defects were shown to enhance spore settlement and reduce the removal of sporelings by hydrodynamic forces from the wrinkled surfaces (Figure 9a). While in uniaxially stretched samples these defects cannot be completely eliminated, some degree of control may still be achieved by fabricating larger specimens and concentrating on areas that are relatively defect/crack-free. We have demonstrated that an alternative way of minimizing structural defects in HWST samples employs biaxial stretching, which, depending on the type of stretching geometry, changes the alignment of wrinkles from parallel to coaxially oriented. Furthermore, the random arrangement of wrinkles is expected to moderate spore settlement behavior and enable areas where settlement was reduced to be identified. The wrinkle geometry does appear to make some difference in the density of settled spores, at least for hydrophobic coatings. In Figure 10 we plot the mean number of spores (per field of view in an optical microscope) as a function of the position on the coating. Specifically, for coatings decorated with tF8H2 SAMs, the density of spores appears to be lower in the middle of the substrate, where the wrinkles are oriented at random. Moving away from the center of the coating, the morphology of the wrinkles changes from random to chevron-like; in this region the number of spores settled on the substrate initially increases and then decreases again as the dimensions of the chevron patterns decrease (Figure 2). However, the settlement of spores on hydrophilic biaxially wrinkled geometries does not seem to depend on the type of dimension of the wrinkling pattern, but this may be masked by the low number of spores that settled on this surface. Clearly additional work is necessary in order to understand the interrelationship between the wrinkle physical dimension and the surface chemistry on settlement and attachment strength of algae and other fouling organisms.

SUMMARY

The results from field and laboratory tests presented and discussed here provide useful insight into the performance of coatings with regard to marine fouling. Barnacle fouling is minimized on topographically corrugated surfaces (even without tuning the surface chemistry), while the settlement and removal of spores and sporelings of *Ulva* is governed by the combination of chemical composition and surface topography. While these conclusions still need to be verified by additional experiments, our results disclose that efficient control of both surface topography and chemistry is important in designing and fabricating an efficient marine coating.

Acknowledgment. We gratefully acknowledge financial support from the Office of Naval Research (Grant No. N00014-07-1-0258 to J.G. and Grant No. N00014-05-1-0134 to J.A.C. and M.E.C.). J.G. and K.E. also thank Microphase Coatings for allowing us to use their field testing facility at Wrightsville Beach, NC. We thank Ben Fletcher for technical assistance with the laboratory assays. We thank Prof. A. B. Brenan for supplying the Silastic T2-coated slides.

REFERENCES AND NOTES

(1) Genzer, J.; Efimenko, K. *Biofouling* **2006**, *22*, 339–360.
(2) Krishnan, S.; Weinman, C. J.; Ober, C. K. *J. Mater. Chem.* **2008**, *18*, 3405–3413.
(3) Kavanagh, C. J.; Quinn, R. D.; Swain, G. W. *J. Adhesion* **2005**, *81*, 843–868.
(4) Hills, J. M.; Thomason, J. C. *Biofouling* **1998**, *12*, 57–69.
(5) Hills, J. M.; Thomason, J. C. *Biofouling* **1998**, *13*, 31–50.
(6) Thomason, J. C.; Le Tissier, M. D. A. A.; Thomason., P. O.; Field, S. N. *Biofouling* **2002**, *18*, 293–304.
(7) Prendergast, G. S.; Zurn, C. M.; Bers, A. V.; Head, R. M.; Hansson, L. J.; Thomason, J. C. *Biofouling* **2008**, *24*, 449–459.
(8) Prendergast, G. S.; Zurn, C. M.; Bers, V.; Head, R. M.; Hansson, L. J.; Thomason, J. C. *: Biofouling* **2009**, *25*, 35–44.
(9) Callow, M. E.; Jennings, A. R.; Brennan, A. B.; Seegert, C. E.; Gibson, A.; Wilson, L.; Feinberg, A.; Baney, R.; Callow, J. A. *Biofouling* **2002**, *18*, 237–245.
(10) Feinberg, A. W.; Gibson, A. L.; Wilkerson, W. R.; Seegert, C. A.; Wilson, L. H.; Zhao, L. C.; Baney, R. H.; Callow, J. A.; Callow, M. E.;

Brennan, A. B.; Clarson, S. J.; Fitzgerald, J. J.; Owen, M. F.; Smith, S. D.; van Dyke, M. E. *Synthesis & Properties of Silicones and Silicon-Modified Materials*; American Chemical Society: Washington, DC, 2003; ACS Symposium Series *838*, pp 196–211.
(11) Hoipkemeirer-Wilson, L.; Schumacher, J.; Carman, M.; Gibson, A.; Feinberg, A.; Callow, M. E.; Finlay, J.; Callow, J. A.; Brennan, A. *Biofouling* **2004**, *20*, 53–63.
(12) Carman, M. L.; Estes, T. G.; Feinberg, A. W.; Schumacher, J. F.; Wilkerson, W.; Wilson, L. H.; Callow, M. W.; Callow, J. A.; Brennan, A. B. *Biofouling* **2006**, *22*, 11–21.
(13) Schumacher, J. F.; Carman, M. L.; Estes, T. G.; Feinberg, A. W.; Wilson, L. H.; Callow, M. E.; Callow, J. A.; Finlay, J. A.; Brennan, A. B. *Biofouling* **2007**, *23*, 55–62.
(14) Schumacher, J. F.; Aldred, N.; Callow, M. E.; Finlay, J. A.; Callow, J. A.; Clare, A. S.; Brennan, A. B. *Biofouling* **2007**, *23*, 307–317.
(15) Bers, A. V.; Wahl, M. *Biofouling* **2004**, *20*, 43–51.
(16) Scardino, A. J.; de Nys, R. *Biofouling* **2004**, *20*, 249–257.
(17) Scardino, A. J.; Harvey, E.; deNys, R. *Biofouling* **2006**, *22*, 55–60.
(18) Howell, D.; Behrends, B. *Biofouling* **2006**, *22*, 401–410.
(19) Chung, K. K.; Schumacher, J. F.; Smapson, E. M.; Burne, R. A.; Antonelli, P. J.; Brennan, A. B. *Biointerphases* **2007**, *2*, 89–94.
(20) Guenther, J.; De Nys, R. *Biofouling* **2007**, *23*, 419–429.
(21) Scardino, A. J.; Guenther, J.; de Nys, R. *Biofouling* **2008**, *24*, 45–53.
(22) Scardino, A. J.; Hudleston, D.; Peng, Z.; Paul, N. A.; de Nys, R. *Biofouling* **2009**, *25*, 83–93.
(23) Efimenko, K.; Wallace, W. E.; Genzer, J. *J. Colloid Interface Sci.* **2002**, *254*, 306–315.
(24) Efimenko, K.; Rackaitis, M.; Manias, E.; Vaziri, A.; Mahadevan, L.; Genzer, J. *Nat. Mater.* **2005**, *4*, 293–297.
(25) Chen, X.; Hutchinson, J. W. *Scr. Mater.* **2004**, *50*, 797–801.
(26) Mahadevan, L.; Rica, S. *Science* **2005**, *307*, 1740.
(27) Callow, M. E.; Callow, J. A.; Pickett-Heaps, J. D.; Wetherbee, R. *J. Phycol.* **1997**, *33*, 938–947.
(28) Finlay, J. A.; Callow, M. E.; Schultz, M. P.; Swain, G. W.; Callow, J. A. *Biofouling* **2002**, *18*, 251–256.
(29) Finlay, J. A.; Fletcher, B. R.; Callow, M. E.; Callow, J. A. *Biofouling* **2008**, *24*, 219–225.
(30) Schultz, M. P.; Finlay, J. A.; Callow, M. E.; Callow, J. A. *Biofouling* **2000**, *15*, 243–251.
(31) Schultz, M. P.; Finlay, J. A.; Callow, M. E.; Callow, J. A. *Biofouling* **2003**, *19*, 17–26 (Supplement).
(32) Chaudhury, M. K.; Finlay, J. A.; Chung, J. Y.; Callow, M. E.; Callow, J. A. *Biofouling* **2005**, *21*, 41–48.
(33) Cassé, F.; Stafslien, S. J.; Bahr, J. A.; Daniels, J.; Finlay, J. A.; Callow, J. A.; Callow, M. E. *Biofouling* **2007**, *23*, 267–276.
(34) Aldred, N.; Clare, A. S. *Biofouling* **2008**, *24*, 351–363.
(35) Swain, G. W.; Nelson, W.; Preedeekanit, W. G. *Biofouling* **1998**, *12*, 257–269.
(36) Bhat, R. R.; Chaney, B. N.; Rowley, J.; Liebmann-Vinson, A.; Genzer, J. *Adv. Mater.* **2005**, *17*, 2802–2807, and references therein.
(37) Guidipati, C. S.; Finlay, J. A.; Callow, J. A.; Callow, M. E.; Wooley, K. L. *Langmuir* **2005**, *21*, 3044–3053.
(38) Krishnan, S.; Ayothi, R.; Hexemer, A.; Finlay, J. A.; Sohn, K. E.; Perry, R.; Ober, C. K.; Kramer, E. J.; Callow, M. E.; Callow, J. A.; Fischer, D. A. *Langmuir* **2006**, *22*, 5075–5086.
(39) Arifuzzaman, S.; Özçam, A. E.; Efimenko, K.; Genzer, J., Work in progress (2009).
(40) The attachment of tF8H2 occurs via a C–O–Si bond that is known to break under extreme pH conditions (see, for instance Spange, S. *Macromol. Symp.* **1998**, *126*, 223). Preliminary tests performed in solutions having various pH ranging from 5–9 indicate, however, that the tF8H2 groups remain present on the surface. We attribute this stability to the formation of in-plane linkages among neighboring tF8H2 groups on the surface.

AM9000562